

## Search for double- $\beta$ decays of tin isotopes with enhanced sensitivity

J. Dawson,<sup>1,2</sup> D. Degering,<sup>3</sup> M. Köhler,<sup>3</sup> R. Ramaswamy,<sup>1</sup> C. Reeve,<sup>1</sup> J. R. Wilson,<sup>1,4</sup> and K. Zuber<sup>1,5</sup>

<sup>1</sup>*Department of Physics and Astronomy, University of Sussex, Falmer, Brighton BN1 9QH, United Kingdom*

<sup>2</sup>*Laboratoire APC, Bâtiment Condorcet, 10, rue Alice Domon et Léonie Duquet, F-75205 Paris Cedex 13, France*

<sup>3</sup>*Verein für Kernverfahrenstechnik und Analytik Rossendorf eV, Postfach 510119, D-01314 Dresden, Germany*

<sup>4</sup>*Department of Physics, University of Oxford, Denys Wilkinson Building, Keble Road, Oxford, OX1 3RH, United Kingdom*

<sup>5</sup>*Institut fuer Kern und Teilchenphysik, Technische Universitaet Dresden, Zellescher Weg 19, D-01069 Dresden, Germany*

(Received 1 April 2008; revised manuscript received 29 July 2008; published 17 September 2008)

A search for the various double- $\beta$  decay modes of  $^{124}\text{Sn}$  and  $^{112}\text{Sn}$  has been performed on 75 kg days of data. New half-life limits for excited states in  $^{124}\text{Sn}$  have been obtained including a lower limit for decay into the first excited  $2^+$  state of  $^{124}\text{Te}$  of  $T_{1/2} > 0.87 \times 10^{20}$  yr (90% C.L.) and into the first excited  $0^+$  state of  $T_{1/2} > 1.08 \times 10^{20}$  yr (90% C.L.). Ground state and excited state transitions of  $^{112}\text{Sn}$  have also been experimentally explored. A limit for the  $2\nu$  EC/EC of  $T_{1/2} > 1.8 \times 10^{19}$  yr (90% C.L.) is obtained. The nonobservation of deexcitation  $\gamma$  from the  $0^+$  at 1888.5 keV results in a lower half-life limit on the  $0\nu$  EC/EC decay of  $^{112}\text{Sn}$  of  $T_{1/2} > 0.8 \times 10^{19}$  yr (90% C.L.), despite a possible resonant enhancement of the decay rate due to degenerated states.

DOI: [10.1103/PhysRevC.78.035503](https://doi.org/10.1103/PhysRevC.78.035503)

PACS number(s): 23.40.Bw, 14.60.Pq, 14.60.St, 27.60.+j

### I. INTRODUCTION

The standard model of particle physics has been extremely successful but is not thought to be the final theory. The quest for physics beyond the standard model is gathering pace, with searches performed at accelerators such as the Tevatron, HERA, and soon at the CERN Large Hadron Collider (LHC). There are also nonaccelerator experiments, such as the search for the rare process known as neutrinoless double- $\beta$  decay.

The classical double- $\beta$  decay is allowed by the standard model. In this reaction, two neutrons in the same nucleus decay simultaneously to emit two antineutrinos and two electrons. This possible reaction was first discussed by M. Goepfert-Mayer [1] in the form of

$$(Z, A) \rightarrow (Z + 2, A) + 2e^- + 2\bar{\nu}_e \quad (2\nu\beta\beta\text{-decay}). \quad (1)$$

As this is a higher order process, to observe this practically requires an isotope in which single- $\beta$  decay is forbidden or strongly suppressed. The energy spectrum from the two electrons has similar features to that from single- $\beta$  decay: a continuous spectrum ending at a well-defined end point determined from the  $Q$  value of the reaction.

The classic papers of Majorana [2], which discuss a two-component neutrino, led Racah [3] and Furry to first discuss a neutrinoless mode in the form of [4]

$$(Z, A) \rightarrow (Z + 2, A) + 2e^- \quad (0\nu\beta\beta\text{-decay}). \quad (2)$$

The signature of this mode is very different to the classical case. Here the summed energy of the two emitted electrons is exactly equal to the  $Q$  value of the reaction. The experimental concept therefore is to observe an isotope capable of decaying via double- $\beta$  decay and to search for a peak at the end point of the spectrum.

This process clearly violates total lepton number conservation by two units and so is forbidden by the standard model. This is in contrast to neutrino oscillations that violate the individual flavor lepton number but conserve the total

lepton number. For this decay to occur, neutrinos must be massive Majorana particles; however any  $\Delta L = 2$  process can contribute to the decay. The most interesting mode is the light Majorana neutrino exchange. Here the measured quantity is known as the effective Majorana neutrino mass, which is given by

$$\langle m_{\nu_e} \rangle = \left| \sum_i U_{ei}^2 m_i \right| = \left| \sum_i |U_{ei}|^2 e^{2i\alpha_i} m_i \right|, \quad (3)$$

which for the case of CP invariance,  $e^{2i\alpha_i} = 0, \pi$ , is

$$\langle m_{\nu_e} \rangle = |m_1 U_{e1}^2 \pm m_2 U_{e2}^2 \pm m_3 U_{e3}^2|. \quad (4)$$

For double- $\beta$  decay, the decay rate and thus inverse half-life is strongly dependent on the available  $Q$  value. In the classic case,  $2\nu\beta\beta$ -decay, the rate is proportional to  $Q^{11}$ , whereas the  $0\nu\beta\beta$ -decay mode scales with  $Q^5$ . For this reason, only high- $Q$ -value decays (typically above 2 MeV) are currently worth studying. This criterion restricts the 35 candidate isotopes to 11.

There are also double- $\beta$  decay modes (both  $2\nu\beta\beta$ -decay and  $0\nu\beta\beta$ -decay) in which  $\gamma$  rays are emitted in addition to the two electrons, thus giving these modes distinct signatures. In principle, a finely segmented detector could observe the two electrons in one segment and simultaneously the emitted  $\gamma$  ray in another segment. Since the energies of the electrons and  $\gamma$  ray are known, this gives a strong experimental signature which is distinct from the background. Studying these modes may shed some light on new physics and provide some new information for nuclear matrix element calculations. Despite their reduced  $Q$  values, there are benefits in studying these modes.

These modes come from two sources: double- $\beta$  decays to excited  $0^+$  and  $2^+$  states of the daughter and double positron decays in which positrons are emitted instead of electrons. Observations of  $2\nu\beta\beta$ -decay transitions into the first excited  $0^+$  state for  $^{100}\text{Mo}$  and  $^{150}\text{Nd}$  have already been reported [5–8].

For the double positron decays, combinations of electron capture (EC) and positron emission can occur:

$$(Z, A) \rightarrow (Z - 2, A) + 2e^+ + (2\nu_e)\beta^+\beta^+, \quad (5)$$

$$e^- + (Z, A) \rightarrow (Z - 2, A) + e^+ + (2\nu_e)\beta^+/\text{EC}, \quad (6)$$

$$2e^- + (Z, A) \rightarrow (Z - 2, A) + (2\nu_e)\text{EC}/\text{EC}. \quad (7)$$

In particular, the  $\beta^+/\text{EC}$  mode shows an enhanced sensitivity to right-handed weak currents [9]. For each positron, there is the possibility of also observing one or both of the 511 keV photons. These modes therefore can provide an extremely clean signature of up to five coincident energy deposits. However, for each generated positron, the available  $Q$  value is reduced by  $2m_e c^2$ , which leads to much smaller decay rates than in comparable  $0\nu\beta\beta$ -decay. For  $\beta^+\beta^+$ -decay to occur, the  $Q$  values must be at least 2048 keV. Only six candidate isotopes are known to have such a high  $Q$  value.

The full  $Q$  value is available only in the EC/EC mode but is difficult to detect. In a neutrinoless EC/EC to the ground state of the daughter, a monoenergetic internal bremsstrahlung must be emitted and requires electron captures of both  $K$  and  $L$  shells. If the initial and final states are degenerate in the context of radiative EC/EC, then a resonant enhancement in the decay rate could occur [10]. The signal observed would come from the deexcitation photons.

The three combinations of electron capture and positron emission have not yet been observed, not even in the neutrino accompanied mode, though there has been a weak indication of the observation of  $^{130}\text{Ba}$  decay in geochemical experiments [11].

There is a wide variety of possible  $\gamma$ -ray emissions. This paper explores those double- $\beta$  transitions of tin isotopes that emit  $\gamma$  rays. There are three double- $\beta$  isotopes of tin:  $^{122}\text{Sn}$  and  $^{124}\text{Sn}$  in the two-electron mode and  $^{112}\text{Sn}$  for  $\beta^+/\text{EC}$  and EC/EC decays. The  $Q$  values of the transition for each of the three isotopes are 366, 2287, and 1922 keV, and the natural abundances are 4.63%, 5.79%, and 0.97%, respectively. As there is no excited state of interest for  $^{122}\text{Sn}$  decay, we focus on the decays

$$^{124}\text{Sn} \rightarrow ^{124}\text{Te} + 2e^- + (2\bar{\nu}_e) + \gamma, \quad (8)$$

$$2e^- + ^{112}\text{Sn} \rightarrow ^{112}\text{Cd} + (2\nu_e) + \gamma, \quad (9)$$

$$e^- + ^{112}\text{Sn} \rightarrow ^{112}\text{Cd} + e^+ + (2\nu_e) + \gamma. \quad (10)$$

$^{124}\text{Sn}$  is one of the 11 isotopes with  $Q$  values larger than 2 MeV, yet there is at present no proposal for a large-scale experiment and few calculations. There are no theoretical predictions of half-lives for  $^{122}\text{Sn}$ . Calculations have been reported for  $2\nu\beta\beta$ -decay ground state transitions in  $^{124}\text{Sn}$ , varying from  $0.7 \times 10^{20}$  to  $3 \times 10^{20}$  yr, and estimates for the first excited states  $0^+$  and  $2^+$  states are  $2.7 \times 10^{21}$  and  $6 \times 10^{26}$  yr, respectively [12,13].

Calculations within the single state dominance model for the  $2\nu\beta^+/\text{EC}$  and  $2\nu\text{EC}/\text{EC}$  ground state transitions in  $^{112}\text{Sn}$  have been made [14]. The half-lives expected are of the order of  $10^{22}$  yr (EC/EC) and  $10^{24}$  yr ( $\beta^+/\text{EC}$ ). However, it is possible that an enhancement of the rate for the  $\beta^+/\text{EC}$  modes occurs as a result of right-handed weak currents.

The radiative neutrinoless EC/EC rate to the ground state of  $^{112}\text{Cd}$  has been estimated to be of the order of  $10^{-29}$  yr $^{-1}$ . This rate may be enhanced by a factor of  $10^6$  by a possible resonance condition [10]. The characteristics of this mode are the monoenergetic internal bremsstrahlung  $\gamma$  at  $Q - E_K - E_L = 1888.5$  keV, with  $E_K$  and  $E_L$  the  $K$ - and  $L$ -shell binding energies of  $^{112}\text{Cd}$ . There could also be a degeneracy between  $^{112}\text{Sn}$  and an excited  $0^+$  state at 1870.9 keV in  $^{112}\text{Cd}$ , which would fulfill the resonance enhancement condition for neutrinoless EC/EC [8].

Two recent studies on tin decays produced half-life limits for various decay modes in the region of  $10^{18}$ – $10^{19}$  yr [15,16]. The aim of this measurement was to improve on those limits, if possible, by another order of magnitude. For this analysis,  $\gamma$  line energies were taken from Ref. [17], and the latest atomic mass determinations from Ref. [18].

## II. EXPERIMENTAL SETUP

The  $\gamma$ -spectrometric measurements were performed in the Felsenkeller underground laboratory near Dresden (Germany) at a depth of 110 mwe (meters of water equivalent). Thirty-six tin bars of 10.6 cm $^2$  area and 4 mm thickness plus four tin sheets of 24.2 cm $^2$   $\times$  3 mm were placed in a Marinelli beaker so that the end cap of the measuring detector was surrounded by the material. The total mass of tin used was 1.24 kg. A passive shielding consisting of 170-mm-thick lead of graded qualities protected the experiment from the ambient background radiation in the measuring chamber. The  $^{222}\text{Rn}$  concentration inside the shielding was reduced by flushing it with gaseous nitrogen. The  $\gamma$  spectrometer used a well-type low-background p-type high-purity Ge detector with 150 cm $^3$  sensitive volume (30% relative efficiency, full width at half maximum (FWHM) at 1.3 MeV: 2.0 keV). For further background suppression, a U-shaped cryostat configuration was applied. Since the muon flux in the laboratory is reduced by a factor of 50 compared to the surface value, no additional active shielding was necessary. The pulse processing electronics used a standard spectrometric amplifier, and the spectrum acquisition was performed by an 8 k channel MCA. Spectra of the tin sample were accumulated during two measuring periods of 598 and 853 h duration. Thus, the total exposure amounted to 74.96 kg days (where the mass refers to natural tin). A blank spectrum of the empty shielding was measured for 762 h.

Just before data collection commenced, the germanium detector was exposed to a mixed source of  $^{241}\text{Am}$ ,  $^{137}\text{Cs}$ , and  $^{60}\text{Co}$ . The  $\gamma$  lines observed from this source were fitted with Gaussian functions. The fitted means were used to accurately calibrate the analog-to-digital converter (ADC) channel to energy relation, and the widths were used to derive a function for the energy resolution (values are given in Table I).

The efficiency and response of the setup was studied using detailed GEANT4 based Monte Carlo simulations, which modeled all parts of the germanium crystal, the crystal housing, the tin pieces, and the background shielding. Samples of  $10^6$   $\gamma$  were simulated inside the tin volume for each energy of interest, and the number of events in the photopeak recorded in the crystal was used to determine the efficiency of observation,

TABLE I. Energy resolution  $\Delta E$  (FWHM),  $\gamma$  detection efficiency  $\epsilon$ , and fitted background  $B$ , for each peak energy. The magnitude of uncertainty in  $\epsilon$  ranges from 0.01% to 0.02%. The background continuum is defined by the polynomial  $B = \alpha + \beta E$  and gives the total counts over the 1451 h of data collected.

| Energy (keV) | $\Delta E$ (keV) | $\epsilon$ (%) | $B$ (counts/keV) |         |
|--------------|------------------|----------------|------------------|---------|
|              |                  |                | $\alpha$         | $\beta$ |
| 553.8        | 1.739            | 3.51           | 476              | -0.62   |
| 602.7        | 1.763            | 3.36           | 425              | -0.49   |
| 606.5        | 1.765            | 3.38           | 477              | -0.60   |
| 617.3        | 1.770            | 3.34           | 533              | -0.69   |
| 694.7        | 1.805            | 3.06           | 295              | -0.29   |
| 695.0        | 1.806            | 3.06           | 303              | -0.30   |
| 713.8        | 1.814            | 3.01           | 418              | -0.48   |
| 722.9        | 1.818            | 3.00           | 377              | -0.42   |
| 815.1        | 1.858            | 2.76           | 167              | -0.13   |
| 851.1        | 1.873            | 2.67           | 139              | -0.10   |
| 1054.0       | 1.953            | 2.31           | 118              | -0.07   |
| 1253.4       | 2.022            | 2.05           | 126              | -0.07   |
| 1488.9       | 2.093            | 1.82           | 166              | -0.10   |
| 1888.5       | 2.184            | 1.49           | 123              | -0.06   |

along with Poissonian uncertainties. Furthermore, known contaminants were simulated to confirm understanding of the shape of the background distribution.

### III. DATA

The obtained spectrum compared against a background run is shown in Fig. 1. Because of the better low-energy behavior of the detector in the Felsenkeller with respect to the one used in Ref. [16], the 46.5 keV line from  $^{210}\text{Pb}$  becomes visible, showing the presence of lead in the tin.  $^{210}\text{Pb}$  decays with a half-life of 22.20 yr via  $^{210}\text{Bi}$  (5.012 days) and  $^{210}\text{Po}$  (138.38 days) to stable  $^{206}\text{Pb}$ . Simulations were used to verify that the  $\beta$  emitter  $^{210}\text{Bi}$  ( $E_{\text{max}} = 1162.1$  keV) is responsible for the bremsstrahlung background below 600 keV.  $^{210}\text{Po}$  undergoes

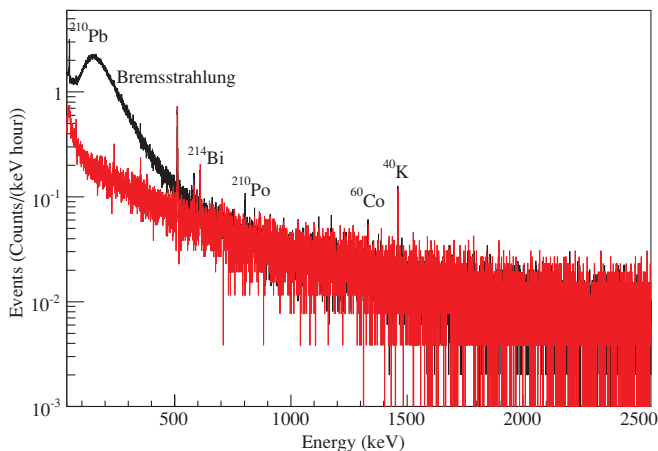


FIG. 1. (Color online) Total spectrum (black), background spectrum (red). A clear bremsstrahlung contribution at lower energies is seen.

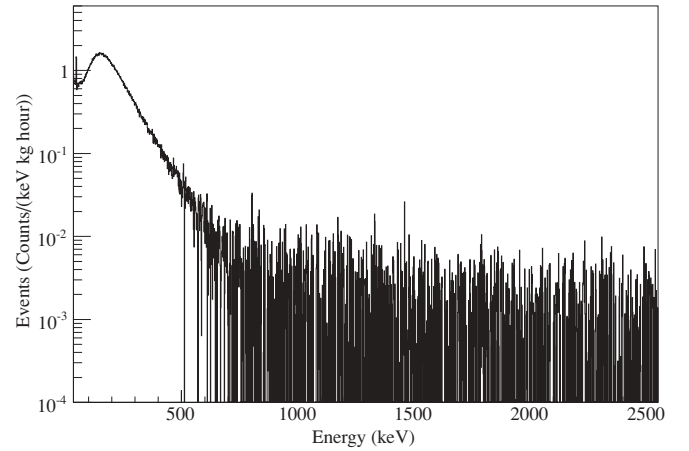


FIG. 2. Background subtracted to reveal the spectrum of the tin sample.

$\alpha$  decay but emits a weak  $\gamma$  line at 803.10 keV which is visible in the tin spectrum. Further contamination from  $^{214}\text{Pb}$  and  $^{214}\text{Bi}$  ( $^{222}\text{Rn}$  successors) as well as  $^{228}\text{Ra}$ ,  $^{228}\text{Th}$ ,  $^{40}\text{K}$ ,  $^{137}\text{Cs}$ , and  $^{60}\text{Co}$  are visible in the tin spectrum at count rates below 0.2 counts/h (Fig. 2).

Weak sawtooth-like features are observed in both tin and background spectra at 693 and 596 keV. These can be attributed to  $^{72,74}\text{Ge}(n, n')$  interactions [19]. The same features were observed more strongly in data collected in a surface laboratory, where the neutron background is expected to be higher, in Ref. [16]. These previous data were used to determine the functional form:

$$f(E) = \kappa [1.0 - 0.04(E - E_0)], \quad (11)$$

when  $E > E_0$  and  $[1.0 - 0.04(E - E_0)] > 0$ ,

$$f(E) = 0 \quad \text{otherwise,}$$

which was found to describe the shape of these features well. Here,  $E_0$  is the starting point of the feature, taken to be 692 and 595 keV for the two separate features observed; whereas  $\kappa$  is the magnitude parameter, which varies with the neutron flux.

### IV. RESULTS

The search performed relies on decays of  $^{124}\text{Sn}$  and  $^{112}\text{Sn}$ . The relevant experimental data, including energy resolution, efficiency, and the background at the energy of each line searched for are compiled in Table I.

#### A. The $^{124}\text{Sn}$ system

A Bayesian analysis approach [20], similar to that described in Ref. [16], was adopted. The most likely values for the magnitude of a linear background component and the amplitude of a Gaussian peak at fixed  $\gamma$  energy were determined from a binned maximum likelihood fit. The mean and width of the  $\gamma$  line under investigation were fixed in the fit, which was carried out over a range of  $\pm 30\sigma$  around the known  $\gamma$

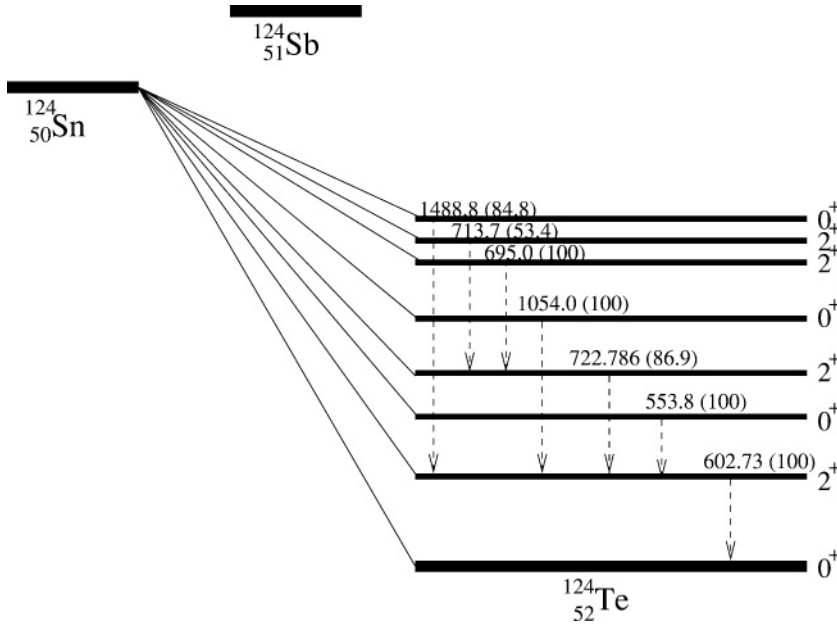


FIG. 3. Level diagram of  $^{124}\text{Sn}$ . The energy of the dominant mode decay  $\gamma$  is given for each level along with the percentage branching ratio in brackets.

energy. When  $\gamma$  lines from known radioactive contaminants fell within this fit range, their amplitudes were also included as fit parameters (again energy and resolution were fixed). The effect of the  $^{72,74}\text{Ge}(n, n')$  interactions at 693 and 596 keV was also included, when relevant, by adding the function in Eq. (11), allowing the parameter  $\kappa$  to vary as a parameter of the fit.

The fitted signal amplitude and uncertainty determined from the likelihood fit,  $\theta_s \pm \delta_s$  was then used to derive a 90% lower limit on the half-life for each decay mode using Eq. (12).

$$T_{\text{half}} \geq \frac{N_{\text{iso}} t_{\text{live}} \epsilon \psi \ln 2}{(\theta_s + 1.28\delta_s)} \quad (\theta_s > 0),$$

$$T_{\text{half}} \geq \frac{N_{\text{iso}} t_{\text{live}} \epsilon \psi \ln 2}{(1.28\delta_s)} \quad (\theta_s \leq 0). \tag{12}$$

Here  $N_{\text{iso}}$  is the number of candidate nuclei in the tin for the given decay,  $t_{\text{live}}$  is the duration of data collection in years,  $\epsilon$  is the efficiency for observing the given  $\gamma$  signal determined from simulations, and  $\psi$  is the branching ratio for the  $\gamma$  line in question. The factor of 1.28 gives one-sided 90% limits. For each fit, the  $\chi^2$  goodness of fit was determined and in all cases indicated good agreement with the data.

The level scheme of  $^{124}\text{Te}$  (given in Fig. 3) shows that the higher level decays all dominantly proceed via the intermediate  $2_1^+$  state at 602.7 keV. Hence, studies of a possible  $\gamma$  peak at 602.7 keV provide information on all these decays. The region of interest about this energy is shown in Fig. 4 along with the fitted signal Gaussian and backgrounds. The efficiency for observing  $\gamma$ 's of this energy from the tin was determined to be  $(3.36 \pm 0.02)\%$  from simulations, and the calculated energy resolution at this point is 1.76 keV (FWHM). With  $1.4 \pm 4.6$  possible events in the Gaussian peak, a half-life of

$$T_{1/2}^{0(2)\nu}(0^+ \rightarrow 2_1^+(602.7 \text{ keV})) > 8.7(11.0) \times 10^{19} \text{ yr} \tag{13}$$

(90(68)% C.L.)

was obtained, an improvement of a factor of 28 on existing limits [16], which can be attributed to the larger size of the germanium detector and the reduced background due to the underground location of this experiment.

Although decays into higher excited states will produce two or more  $\gamma$ 's, it is unlikely that they will all be emitted in the direction of the detector, and therefore, studies of higher states were performed by searching separately for the accompanying  $\gamma$ 's. The fitted events and derived half-life limits for these decays are compiled in Table II. The branching ratio for the deexcitation chain, which is given in Fig. 3 and can be less than 100% for the higher excited states, was included in the calculation of half-life. In some cases, the best limit on half-life is derived from one of the lower deexcitation steps in the decay chain (indicated by a † in the table).

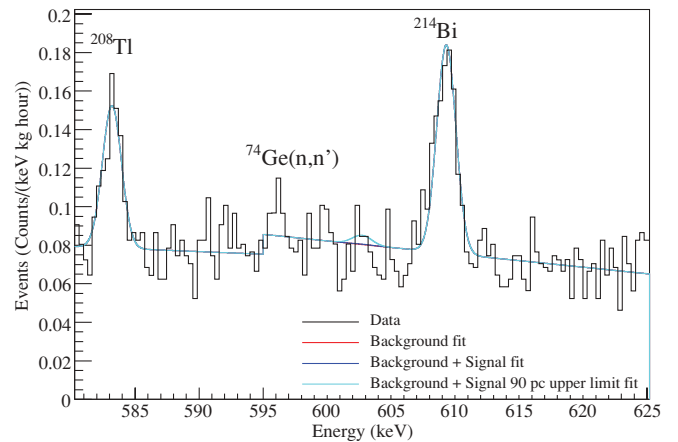


FIG. 4. (Color online) Peak range around 602.7 keV. Natural radioactivity from  $^{208}\text{Tl}$  and  $^{214}\text{Bi}$  produces the lines at 583 and 609 keV, respectively.

TABLE II. Half-life limits (90% C.L.) for all possible excited  $0^+$ ,  $2^+$  state transitions ( $0\nu$  and  $2\nu$ ) of  $^{124}\text{Sn}$ . Given are the excited states, all possible  $\gamma$  lines with the dominant mode searched for in bold, the total number of fitted events in the peak, and deduced half-life limits. For decays marked  $\dagger$  the better half-life limit of the 602.7 keV  $\gamma$  in the first row applies.

| Excited state    | $\gamma$ energy (keV)       | Events           | $T_{1/2}$ ( $10^{20}$ yr) |
|------------------|-----------------------------|------------------|---------------------------|
| $2_1^+$ (602.7)  | <b>602.7</b>                | $0.6 \pm 12.3$   | 0.87                      |
| $0_1^+$ (1156.5) | <b>553.8</b> , 602.7        | $-44.4 \pm 10.6$ | 1.08                      |
| $2_2^+$ (1325.5) | <b>722.9</b> , 602.7        | $6.5 \pm 8.8$    | $0.62\dagger$             |
| $0_2^+$ (1656.7) | <b>1054.0</b> , 602.7       | $-1.8 \pm 6.7$   | 1.13                      |
| $0_3^+$ (2020.0) | <b>695.0</b> , 722.9, 602.7 | $18.1 \pm 12.1$  | $0.38\dagger$             |
| $2_2^+$ (2039.3) | <b>713.8</b> , 722.9, 602.7 | $-8.1 \pm 8.5$   | $0.62\dagger$             |
| $2_3^+$ (2091.6) | <b>1488.9</b> , 602.7       | $-9.0 \pm 4.7$   | 1.08                      |

### B. The $^{112}\text{Sn}$ system

The second system to analyze is  $^{112}\text{Sn}$ , which has the decay level scheme shown in Fig. 5. It offers a more complex search pattern as in addition to the deexcitation  $\gamma$ 's more photons can be emitted in the EC/EC or  $\beta^+$ /EC process.

Again, all decays into higher excited states proceed via a  $2_1^+$  state, this time at 617.3 keV. Thus, a search for this line places a half-life limit on all excited state transitions, taking into account the branching ratios of the deexcitation. Figure 6 shows the fitted region where no peak was observed, resulting in a half-life limit of

$$T_{1/2}^{0(2)\nu\text{EC/EC}+\beta^+/\text{EC}}(0^+ \rightarrow 2_1^+(617.6 \text{ keV})) > 1.8 \times 10^{19} \text{ yr} \quad (90\% \text{ C.L.}) \quad (14)$$

Decays to excited states were treated in a similar manner to the  $^{124}\text{Sn}$  system. The results of searches for all the potential  $\gamma$  lines and the derived half-life limits are compiled in Table III.

TABLE III. Half-life limits (90% C.L.) for excited state transitions ( $0\nu$  and  $2\nu$ ) of  $^{112}\text{Sn}$ . Given are the excited states, all possible  $\gamma$  lines with the dominant mode searched for in bold, the total number of fitted events in the peak, and deduced half-life limits. For decays marked  $\dagger$  the better half-life limit of the 617.3 keV  $\gamma$  in the first row applies.

| Excited state    | $\gamma$ energy (keV) | Events          | $T_{1/2}$ ( $10^{19}$ yr) |
|------------------|-----------------------|-----------------|---------------------------|
| $2_1^+$ (617.3)  | <b>617.3</b>          | $-5.4 \pm 10.1$ | 1.8                       |
| $0_1^+$ (1224.1) | <b>606.5</b> , 617.3  | $-1.1 \pm 10.4$ | 1.8                       |
| $2_2^+$ (1312.3) | <b>694.7</b> , 617.3  | $15.2 \pm 12.1$ | $0.5\dagger$              |
| $0_2^+$ (1433.2) | <b>815.8</b> , 617.3  | $8.3 \pm 8.0$   | $0.7\dagger$              |
| $2_3^+$ (1468.7) | <b>851.1</b> , 617.3  | $-0.5 \pm 7.4$  | $1.3\dagger$              |
| $0_3^+$ (1870.9) | <b>1253.4</b> , 617.3 | $-5.0 \pm 5.8$  | $1.7\dagger$              |

Decay to the  $0^+$  state at 1870.9 keV is particularly interesting, as this state could be degenerate with the ground state of  $^{112}\text{Sn}$ , which could result in a resonantly enhanced neutrinoless EC/EC rate. Deexcitation of this state is dominated by the emission of a 1253.4 and 617.3 keV  $\gamma$ . No obvious peak was observed at either of these energies, resulting in a half-life limit on this decay mode of

$$T_{1/2}^{0(2)\nu\text{EC/EC}}(0^+ \rightarrow 0^+(1870.9 \text{ keV})) > 1.8 \times 10^{19} \text{ yr} \quad (90\% \text{ C.L.}) \quad (15)$$

The  $\beta^+$ /EC modes can only populate excited states up to  $Q - 1.022$  MeV, which corresponds to levels below 900 keV for  $^{112}\text{Sn}$ . Only the  $2_1^+$  state at 617.3 keV satisfies this criterion. Therefore the half-life limit from the 617.3 keV line search for EC/EC, given in Eq. (14), also applies to the  $0(2)\nu$   $\beta^+$ /EC-decay modes into the first excited  $2_1^+$  state.

A search was also performed for the  $0\nu$  EC/EC ground state transition, based on the emission of an internal bremsstrahlung photon [21]. Because of energy and momentum conservation, this requires one  $K$ - and one  $L$ -shell capture. Additionally,

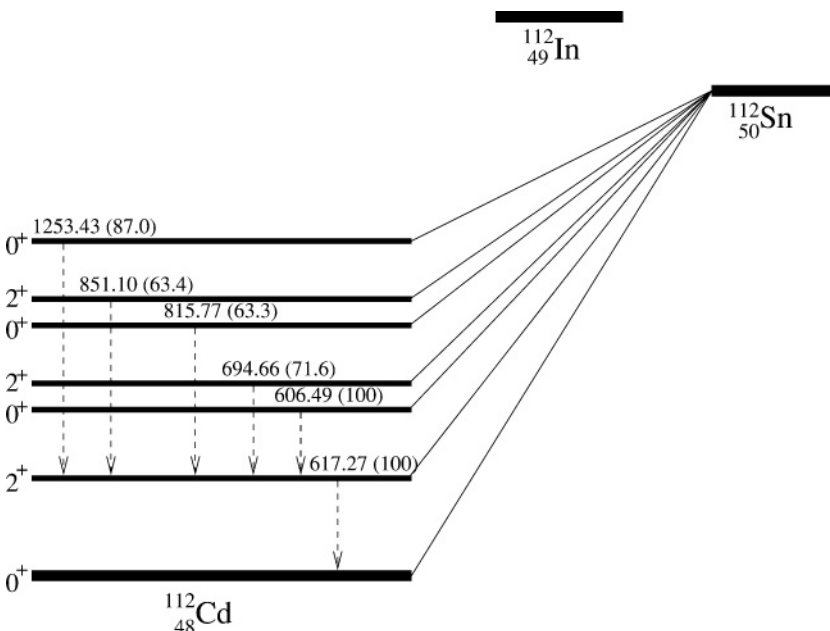


FIG. 5. Level diagram of  $^{112}\text{Sn}$ . The energy of the dominant mode decay  $\gamma$  is given for each level along with the percentage branching ratio in brackets.

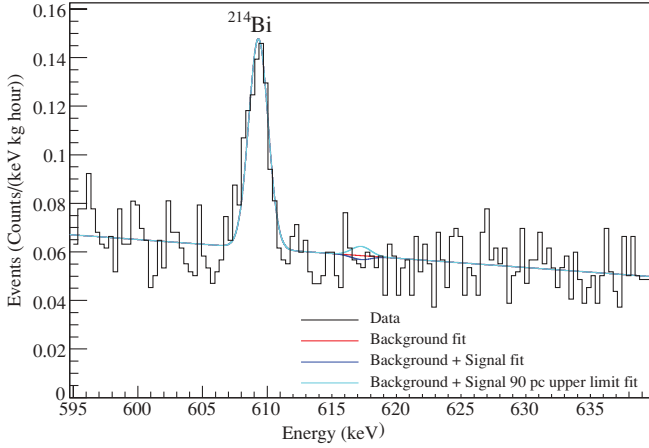


FIG. 6. (Color online) Data in the range around 617.3 keV. The line at 609.3 keV stems from  $^{214}\text{Bi}$  decay in the natural  $^{238}\text{U}$  decay chain.

the bremsstrahlung photon has to be monoenergetic, with an energy of the  $Q$  value reduced by the  $K$ - and  $L$ -shell binding energy of the daughter. In the case of  $^{112}\text{Sn}$  this implies a  $\gamma$  of 1888.5 keV. The calculated detection efficiency for such a photon is  $(1.491 \pm 0.013)\%$ . Figure 7 shows the energy region for this search, which resulted in a half-life limit of

$$T_{1/2} > 2.0 \times 10^{19} \text{ yr (90\% C.L.)} \quad (16)$$

due to the nonobservation of a peak. Uncertainties in the atomic masses mean that the peak position is only known to about  $\pm 2$  keV [18]. Therefore, the peak position was systematically varied by 0.5 keV between 1886 and 1890 keV, and the fit was repeated for the corresponding position. The conservative lower limit for this decay is taken as

$$T_{1/2}^{0\nu\text{EC/EC}}(0^+ \rightarrow 0_{g.s.}^+) > 0.8 \times 10^{19} \text{ yr (90\% C.L.)}, \quad (17)$$

the worst half-life limit found in this range.

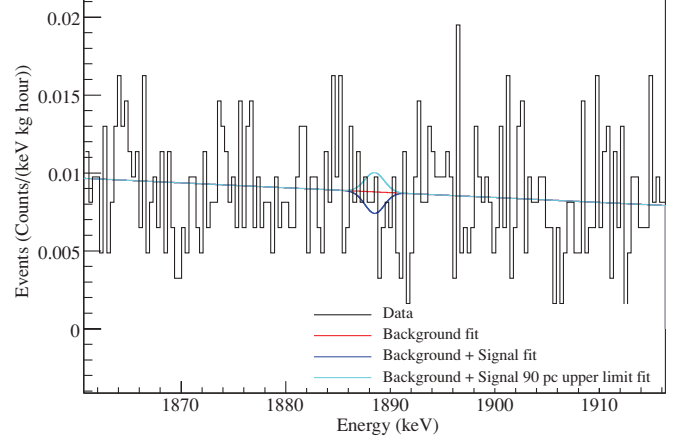


FIG. 7. (Color online) Data around 1888.5 keV, and the fitted peak limits.

## V. SUMMARY AND CONCLUSIONS

Double- $\beta$  decay, in its various forms, is a powerful tool for investigating neutrino properties. Although it has received little interest in the field so far, tin presents two isotopes of interest:  $^{124}\text{Sn}$  which is suitable for  $0\nu\beta^-\beta^-$  searches and  $^{112}\text{Sn}$  available for decay via the  $\beta^+/\text{EC}$  mode. In this paper, new half-life limits are presented for various decays of these two isotopes, based on the nonobservation of characteristic  $\gamma$  lines. All of the limits presented here improve on previous values given in Ref. [16] by an order of magnitude or more. With limits of order  $10^{20}$  yr for a number of decay modes, this paper might trigger some new theoretical efforts to calculate  $2\nu\beta\beta$ -decay half-lives in the tin systems. During submission of this paper, we became aware of a similar study in Ref. [22].

## ACKNOWLEDGMENTS

We thank V. I. Tretyak for useful discussion and B. Morgan and Y. Ramachers for software. J. R. Wilson acknowledges support from the Leverhulme Trust.

- 
- [1] M. Goepfert-Mayer, Phys. Rev. **48**, 512 (1935).  
 [2] E. Majorana, Nuovo Cimento **14**, 171 (1937).  
 [3] G. Racah, Nuovo Cimento **14**, 322 (1937).  
 [4] W. Furry, Phys. Rev. **56**, 1184 (1939).  
 [5] A. S. Barabash *et al.*, Phys. Lett. **B345**, 408 (1995).  
 [6] A. S. Barabash *et al.*, Phys. At. Nucl. **67**, 1216 (2004).  
 [7] R. Arnold *et al.*, Nucl. Phys. **A781**, 209 (2007).  
 [8] A. S. Barabash, AIP Conf. Proc. **942**, 8 (2007).  
 [9] M. Hirsch *et al.*, Z. Phys. A **347**, 151 (1994).  
 [10] Z. Sujkowski and S. Wycech, Phys. Rev. C **70**, 052501(R) (2004).  
 [11] A. P. Meshik, C. M. Hohenberg, O. V. Pravdivtseva, and Y. S. Kapusta, Phys. Rev. C **64**, 035205 (2001).  
 [12] E. Caurier, F. Nowacki, A. Poves, and J. Retamosa, Nucl. Phys. **A654**, 973c (1999).  
 [13] M. Aunola and J. Suhonen, Nucl. Phys. **A602**, 133 (1996).  
 [14] P. Domin *et al.*, Nucl. Phys. **A753**, 337 (2005).  
 [15] H. J. Kim *et al.*, Nucl. Phys. **A793**, 171 (2007).  
 [16] J. Dawson *et al.*, Nucl. Phys. **A799**, 167 (2008).  
 [17] *Table of Isotopes*, 8th ed., edited by R. Firestone, C. M. Baglin, and S. Y. Frank Chu (Wiley, New York, 1999).  
 [18] G. Audi, A. H. Wapstra, and C. Thibault, Nucl. Phys. **A729**, 337 (2003).  
 [19] D.-M. Mei, S. R. Elliot, A. Hime, V. Gehman, and K. Kazkaz, Phys. Rev. C **77**, 054614 (2008).  
 [20] W.-M. Yao *et al.*, J. Phys. G: Nucl. Part. Phys. **33**, 1 (2006).  
 [21] M. Doi and T. Kotani, Prog. Theor. Phys. **89**, 139 (1993).  
 [22] A. S. Barabash *et al.*, Nucl. Phys. **A807**, 269 (2008).